Cancer Letters 460 (2019) 128–138

Contents lists available at ScienceDirect

Cancer Letters

journal homepage: www.elsevier.com/locate/canlet

hsa_circ_0091570 acts as a ceRNA to suppress hepatocellular cancer progression by sponging hsa-miR-1307

Yu-Gang Wang[a,1], Tao Wang[b,1], Min Ding[b], Shi-Hao Xiang[a], Min Shi[a,**], Bo Zhai[b,*]

[a] Department of Gastroenterology, Tongren Hospital, Shanghai Jiao Tong University School of Medicine, Shanghai, China
[b] Department of Interventional Oncology, Renji Hospital, School of Medicine, Shanghai Jiaotong University, Shanghai, China

ARTICLE INFO

Keywords:
Hepatocellular cancer
circRNA
hsa_circ_0091570
miR-1307
Competing endogenous RNA

ABSTRACT

Alterations in circular RNA (circRNA) expression have a vital impact on the biological processes in cancer. Moreover, the expression pattern and roles of circRNAs in hepatocellular cancer (HCC) remain unclear. This study performed qRT-PCR to determine the regulated circRNAs in HCC tissues and cell lines. CCK8, 5-ethynyl-2′-deoxyuridine (EdU) assay, colony formation, cell cycle assay, apoptotic assay, transwell, and wound healing assay were conducted to assess the function of hsa_circ_0091570 or miR-1307 on cell proliferation, apoptosis, and migration in vitro. Mouse xenograft models were used to measure the functions of hsa_circ_0091570 in vivo. The decreased expression of hsa_circ_0091570 was associated with the pathological staging of HCC patients. Furthermore, inhibition of hsa_circ_0091570 promoted cell proliferation and migration, blocked cell apoptosis in HCC cell lines, and promoted tumor growth in the mouse xenograft model. RNA immunoprecipitation assay verified the interaction of hsa_circ_0091570 and miR-1307. The miR-1307 inhibitor inhibited the function induced by hsa_circ_0091570 siRNA. Overall, hsa_circ_0091570 sponge miR-1307 as a ceRNA and regulate ISM1 expression by exerting functional roles in HCC.

1. Introduction

Hepatocellular carcinoma (HCC) is a common malignant tumor and is one of the main causes of cancer-related deaths worldwide [1]. Global HCC deaths have reached 700,000 annually [2]. Viruses, chemicals, and inborn or acquired metabolic diseases are all factors responsible for HCC development [3]. HCC patients are usually diagnosed during the advanced stages [4]. Various therapies have been used to treat liver cancer, but HCC prognosis remains poor, with a five-year survival of less than 20%, due to its high frequency of metastasis and recurrence [5,6]. Meanwhile, no clinical biomarker is available to sensitively and specifically diagnose HCC [7]. Thus, the pathogenesis and possible therapeutic targets of HCC should be investigated.

Circular RNA (circRNA), a non-coding RNA, is characterized by a covalently closed loop without 5′ to 3’ polarity and polyadenylated tail [8]. Studies have shown that circRNAs participate in various physiological and pathological processes, such as growth, differentiation, and metastasis, of cancer cells [9,10]. In HCC, some circRNAs have been indicated in tumor progression [11–13]. Hsa_circ_0103809 promotes cell proliferation and inhibits apoptosis in HCC by targeting the miR-490-5p/SOX2 signaling pathway [11]. Moreover, hsa_circ_0128298 is a biomarker for the diagnosis and prognosis of HCC [14]. Uncovering the role of circRNAs in HCC will improve our understanding of the molecular mechanisms of HCC carcinogenesis.

MiRNAs are short noncoding RNAs that bind to the 3′-untranslated regions (UTRs) of the target genes that are involved in multifarious cellular processes to silence their expressions [15]. Moreover, dysregulated circRNAs in cancer can serve as competing endogenous RNAs (ceRNAs) or miRNA sponges, which interact with RNA binding proteins, to modulate the mRNA stability [16,17]. The ceRNA network has revealed a new mechanism of interaction between RNAs. A miRNA can bind to mRNA 3′UTR via microRNA response elements (MREs), resulting in mRNA degradation or translation inhibition. Other RNAs form a ceRNA when they have the same MRE as the mRNA, which indirectly regulates the expression level of mRNAs and affect cell function [18]. CircRNA8924 is a ceRNA involved in cervical cancer

* Corresponding author. Department of Interventional Oncology, Renji Hospital, School of Medicine, Shanghai Jiaotong University, 106 Pujian Road, 200127, Shanghai, China.
** Corresponding author. Department of Gastroenterology, Tongren Hospital, Shanghai Jiao Tong University School of Medicine, 1111 Xianxia Road, 2000336, Shanghai, China.
E-mail addresses: shimingdyx@163.com (M. Shi), zhaiboshi@sina.com (B. Zhai).
[1] The authors contributed equally to this study.

https://doi.org/10.1016/j.canlet.2019.06.007
Received 11 February 2019; Received in revised form 10 June 2019; Accepted 11 June 2019

progression by competitively binding to the miR-518d-5p/519-5p family [10]. CircRNA hsa_circ_0008039, as a ceRNA of miR-432-5p, can promote breast cancer cell proliferation and migration [19]. However, the expression and function of circRNAs in HCC have been rarely investigated. This research investigates the possible role and the molecular mechanism of hsa_circ_0091570 in HCC.

In this study, we analyzed the expression profile of circRNAs in HCC tissues. The expression level of hsa_circ_0091570 was remarkably down-regulated in HCC tissues and cell lines. The expression of hsa_circ_0091570 showed considerably correlation with the prognosis of HCC patients. Moreover, down-regulation of hsa_circ_0091570 promoted cell proliferation and migration and suppressed apoptosis. The hsa_circ_0091570 was showed to bind to miR-1307, as shown by RNA immunoprecipitation (RIP) assay. Additionally, ISM1 was directly targeted by miR-1307. In summary, hsa_circ_0091570 competitively bound to miR-1307 by acting as a ceRNA and regulated ISM1 expression. hsa_circ_0091570 serve as a new biomarker for HCC prognosis and may be a potential therapeutic target for HCC patients.

2. Materials and methods

2.1. Microarray processing

The expression profiles of circRNAs in seven pairs of tissue samples (7 HCC tissues and 7 matched para-carcinoma normal tissues) were analyzed by using a microarray GSE97332 from GPL19978 platform.

2.2. Clinical specimens

A total of 60 pairs of HCC tissues and matched para-carcinoma normal tissues were obtained from patients who underwent surgery at Renji Hospital between 2011 and 2017, and were confirmed by pathological examination. Written informed consent was obtained before the research. All the specimens (60 HCC tissues and 60 non-tumor matched tissues) were stored at −80 °C for investigation. Tumor staging was based on a lymph node metastasis (TNM) staging system. This research was approved by the Ethics Committees of Renji Hospital (Clinical Research Ethics Approval No. 2013(22)). Clinical data of patients are summarized in Table 1.

2.3. Cell culture and transfection

Human HCC cell lines (HepG2 and SMMC-7721) and normal liver cell lines (LO2) were purchased from American Type Culture Collection (ATCC, USA) and cultured in DMEM (Invitrogen, USA) with 10% FBS (GIBCO, Brazil) at 37 °C with 5% CO_2. Small interfered RNAs (hsa_circ_0091570 siRNA), miR-1307 mimics, miR-1307 inhibitors, and their negative controls were transfected into cells by using Lipofectamine 2000 (Invitrogen, USA) based on the manufacturer's instructions.

2.4. RNA extraction and qRT-PCR

RNA extraction of tissues and cells was performed by using a TRIzol reagent (Invitrogen, Carlsbad, CA, USA). PrimeScript RT reagent kit (Takara Bio Inc, China) was used to obtain cDNA. qPCR was conducted by using a SYBR PremixEx Taq (Vazyme, China) to measure the abundance of transcripts. All qRT-PCR assays were performed at least thrice. All the primers in this study were expressed as follows: hsa_circ_0091570: F: 5′-CTACACCTACCACTGTGTCTGC-3′, R:5′-AAGCCATGGGAGGATTAGCTG-3′; ISM1: F: 5′-CTTCCCCAGACCGCGATTC-3′, R: 5′- CGACCACCTCTATGGTGACCT-3′; miR-1307: F: 5′- ACACTCCAGCTGGGACTCGGCGTGGCGTCG-3′, R: 5′- CTCAACTGGTGTCGTGGAGTCGGCAATTCAGTTGAGCACGACCG -3′. The primers were synthesized by Invitrogen (Shanghai, China).

Table 1
Patient cohort description.

Feather	Number	Low	High	P value
All cases	60	30	30	
Age(years)				0.6023
< 60	34	18	16	
≥60	26	12	14	
Gender				0.5186
Male	48	25	23	
Female	12	5	7	
Tumor size (cm)				**0.0025**
< 3	16	3	12	
3-5	13	5	9	
> 5	31	22	9	
Differentiation grade				**0.0001**
Well	6	0	7	
Moderate	29	10	18	
Poorly	25	20	5	
Tumor number				0.6048
Solitary	28	13	15	
Multiple	32	17	15	
Tumor capsular				0.3132
Incomplete	1	1	0	
Complete	59	29	30	
WHO stage				**0.0035**
I ~ II	16	3	13	
III ~ IV	44	27	17	

Total data from 60 HCC patients were analyzed. For the expression of hsa_circ_0091570 was assayed by qRT-PCR, the median expression level was used as the cutoff. Data were analyzed by chi-squared test. P-value in bold indicates statistically significant.

2.5. RNase R digestion

RNase R (3 U/ug) (Epicenter Biotechnologies) was incubated with total RNA (5 μg) for 15 min at 37 °C. This reaction was performed twice in accordance with previously published procedures.

2.6. Sanger sequencing

Sanger sequencing by Realgene (Nanjing, China) was used to determine the amplification products of circRNAs. The primers are listed as follows: (hsa_circ_0091570: 5′- CTACACCTACCACTGTGTCTGC-3′ (sense) and 5′- AAGCCATGGGAGGATTAGCTG-3′ (antisense)).

2.7. Luciferase reporter assay

After seeding into 24-well plates, cells (1 × 10∧4) were co-transfected with luciferase reporter (10 ng) and miR-1307 mimics (80 nM) or NC using Lipofectamine 2000 (Invitrogen). A dual-luciferase reporter assay system (Promega) was used to perform the luciferase reporter assay.

2.8. RIP

Magna RIP RNA-Binding Protein Immunoprecipitation Kit (Millipore, Bedford, MA, USA) was used to perform the RIP experiment. The RIP procedure was based from a previous study [20]. The mixture was applied for RNA extraction and detection.

2.9. Western blot analysis

RIPA lysis buffer (Keygen Biotech) was used for total protein extraction. The extracted protein was run on 10% acrylamide gel SDS-PAGE and transferred to PVDF membranes (Bio-Rad, Hercules, California, USA). After blocking, the PVDF membranes were incubated with specific primary antibodies for 24 h at 4 °C. After washing for five times using TBST, the membranes were incubated with the secondary

antibody for 1 h. The proteins were visualized through a chemiluminescent reaction (ECL, Beyotime, Shanghai, China). Semi-quantitative analysis was performed on Image Lab.

2.10. Cell cycle assay

After treatment, cells were collected and mixed with 70% ethanol at 4 °C overnight. Subsequently, 100 μl RNase A (Keygen Biotech, Nanjing, China) was added to the mixture. After incubation at 37 °C for 30 min, cells were stained with 400 μl propidium iodide (Keygen Biotech) for 30 min. The samples were examined by using a flow cytometer FACSCalibur (BD Biosciences, San Jose, CA, USA).

2.11. Apoptotic assay

Transfected cells were harvested in flow tubes and washed with cool PBS and 1 × binding buffer thrice. Annexin V-FITC Apoptosis Detection Kit (Vazyme, Nanjing, China) was used to stain the cells, and flow cytometry (FACScan, BD Biosciences, USA) was used to analyze the apoptotic rate of cells.

2.12. Cell proliferation assay

The proliferation rate of cells was measured by using CCK-8 assay (Dojindo Laboratories, Japan). The absorbance was measured at 450 nM by using a SpectraMax 250 spectrophotometer (Molecular Devices, USA). The procedure followed previously published methods [10].

EdU assay (Ribobio, Guangzhou, China) was used to determine the cell proliferative capacity. The cells (10∧4) in a logarithmic state were seeded into 96-well plates. All operations were performed based on instructions. Fluorescence microscopy was conducted to acquire and analyze the images. All the experiments were performed for at least thrice.

2.13. Colony formation assay

The cell was diluted to 1 × 10∧3/mL, and 200 u L cell suspension was seeded into the plate (200 cells in each dish) and cultured for 2 weeks. Cell culture was halted until visible clone formation. Methanol (5 ml) was fixed for 15 min, followed by Giemsa for 20 min. After washing, the number of clones was counted by using the transparent film of the grid. Afterward, colony formation assay rate was calculated and photographed.

2.14. Wound healing assay

Scratch wound healing and transwell system was used to measure cell migration. The cells were seeded on 6-well plates and scratched with a 10 μl pipette tip. After washing thrice, the non-adherent cells were washed. Cell migration toward the wound 24 h post-scratching was photographed by using an inverted microscope (Olympus, Japan), and the total wound areas were analyzed on Image J to assess migration capacity.

2.15. Cell migration and invasion assays

The transwell system was used to determine cell migration. Migration: HCC cells were seeded into the upper compartment of the chamber. Invasion: The transwell chamber was coated with Matrigel diluted with a serum-free medium at the bottom of the upper chamber before adding HCC cells into the upper compartment of the chamber. After incubation at 37 °C for 24 h, the cells on the lower surface of the chamber were mixed with methanol and stained with 0.1% crystal violet. Non-migrating cells were wiped with a cotton swab, and 5 randomly selected fields were photographed and counted per well. Each experiment was repeated thrice.

2.16. Mouse xenograft model

BALB/c nude mice received subcutaneous injections of 2 × 10∧6 HepG2 cells (hsa_circ_0091570 over-expression plasmid, siRNA or negative control). Tumor volumes were measured every 4 days. The following formula: volume = length × $(width/2)^2$ was used to calculate tumor volume. The study was approved by the Ethics Committee of Shanghai Tongren Hospital, Shanghai Jiao Tong University School of Medicine, and the experiments followed the rules on animal welfare and NIH requirements.

2.17. Metastasis assays

HepG2 cells with diverse treatment were injected into nude mice via the tail vein. The mice were harvested after 28 days. Lung metastatic nodules were counted to determine the metastasis of cells with different treatments. HE staining was used to confirm the metastatic tumors.

2.18. HCC-bearing nude mice

Human HCC-bearing male nude mice with the subcutaneous passage of SMMC-LTNM were used to evaluate the effect of hsa_circ_0091570. The mice model was assessed based on previous instructions [21]. During the research, 10 nmol RNA in a 0.1 ml saline buffer was injected into the tumor mass every 3 days for 2 weeks. The serum AFP levels of mice were detected by using ELISA at 2 weeks pre- and post-injection. At 2-week post-injection, the immunohistochemistry of the tumor mass was analyzed. The study was approved by the Ethics Committee of Shanghai Tongren Hospital, Shanghai Jiao Tong University School of Medicine, and the experiments were performed based on the rules on animal welfare and NIH requirements.

2.19. Immunohistochemistry

Tissue sections were incubated with antibodies against ISM1 (CST), MMP2 (CST), or PCNA (CST) at 4 °C overnight. All the procedures were performed, as previously reported [22].

2.20. Statistical analysis

Data was presented as means ± standard deviation and were analyzed by using SPSS 19.0. Student's t-test was used for difference analysis between the two groups, and $P < 0.05$ was the significant criteria. All experiments were repeated more than thrice.

3. Results

3.1. Characterization and expression of hsa_circ_0091570 in HCC

Microarray GSE97332 was used to analyze the alterative expression profiles of circRNAs in seven pairs of tissue samples (7 HCC tissues and 7 matched tissues). Among these significantly regulated circRNAs, hsa_circ_0091570 was selected as a candidate circRNA. qRT-PCR was performed to amplify hsa_circ_0091570 in HCC tissue samples. Sanger sequencing was used to confirm the amplified product of hsa_circ_0091570, and the sequence was the same as that in CircBase (Fig. 1A). RNase R enzyme had no effect on circRNAs compared with linear RNAs, and this finding determined the circRNA characteristics of hsa_circ_0091570 (Fig. 1B). The expression levels of hsa_circ_0091570 were determined via qRT-PCR of another 60 pairs of tissue samples (60 HCC tissues and 60 non-tumor matched tissues). Thus, hsa_circ_0091570 was significantly down-regulated in HCC tissues compared with matched non-tumor tissues (Fig. 1C). Furthermore, the relationship between hsa_circ_0091570 expression and clinic pathological

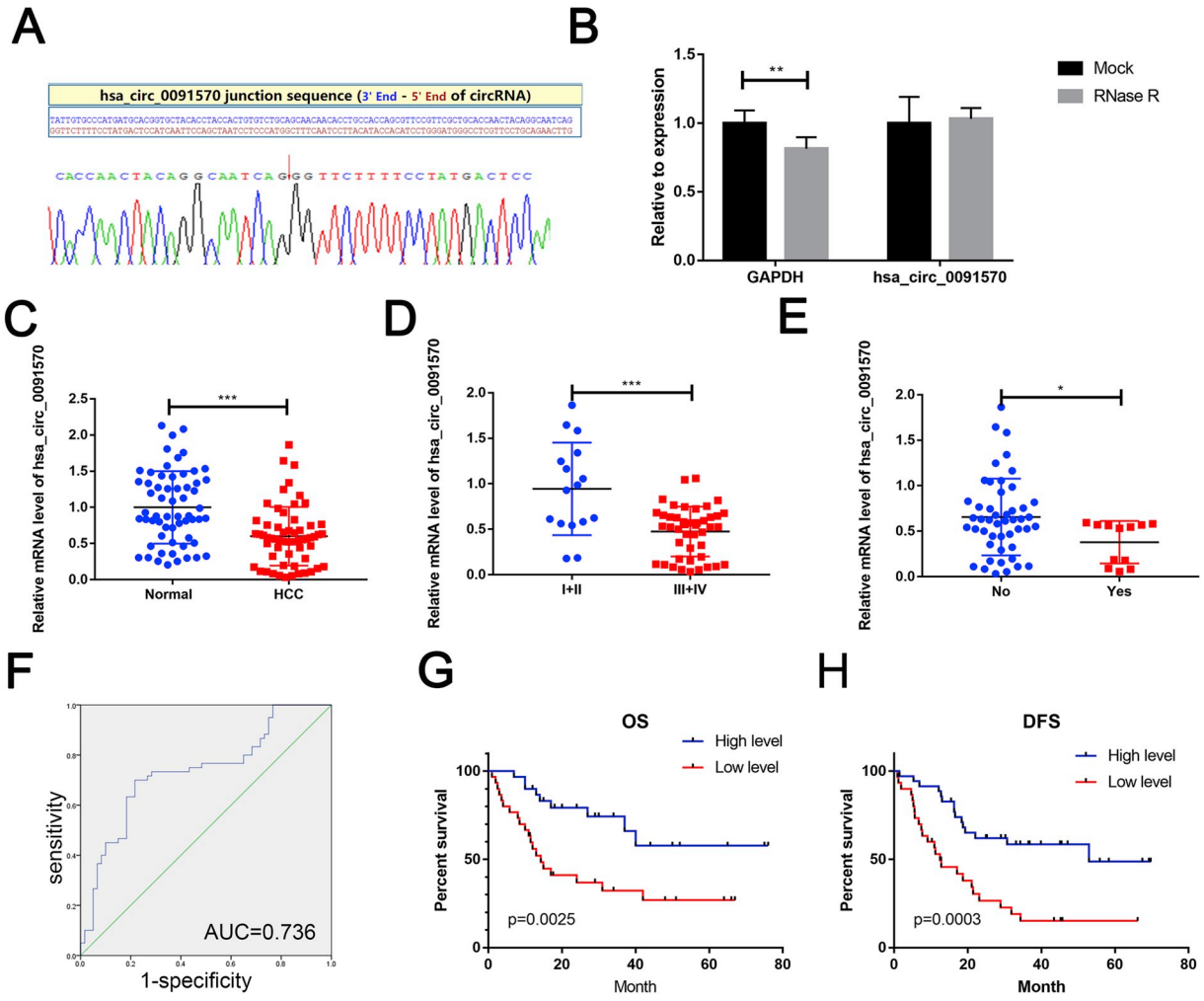

Fig. 1. Characterization and expression of hsa_circ_0091570 in HCC. A: Sequence of hsa_circ_0091570 in circBase (upper part) is consistent with Sanger sequencing (lower part). B: Circular RNA is resistant to RNase R treatment in HepG2 cell lines. C: Expression of hsa_circ_0091570 in HCC tissues and paired para cancerous tissues (n = 60). hsa_circ_0091570 is significantly reduced in tumor tissues. D: Expression level of hsa_circ_0091570 is positively correlated with the tumor grade in HCC. E: Expression level of hsa_circ_0091570 is positively correlated with portal vein tumor thrombus in HCC. F: ROC curve of hsa_circ_0091570 to distinguish HCC from controls. G and H: Kaplan–Meier analyses of the associations among the hsa_circ_0091570 expression level, overall survival (G), and disease-free survival (H) of patients with HCC (log-rank test is used to calculate the p-values).

parameters were evaluated. The results indicated that the decreased expression of hsa_circ_0091570 is associated with the high Edmondson Grade and portal vein tumor thrombus (Fig. 1D and E). For the role of circRNAs as biomarkers of different diseases, receiver operating characteristic (ROC) curve analysis was conducted to assess the diagnostic sensitivity and specificity of hsa_circ_0091570 for HCC. The area under the curve was 0.736, which shows that hsa_circ_0091570 has a potential diagnostic capability (Fig. 1F). In addition, hsa_circ_0091570 was related to overall survival rates (Fig. 1G and H).

3.2. hsa_circ_0091570 regulated cell proliferation, cell apoptosis, cell cycle, and cell migration

To determine the functional role of hsa_circ_0091570, we detected the expression of hsa_circ_0091570 in human HCC cell lines (7402, 97H, HepG2, and SMMC-7721) and normal liver cell lines (LO2). The expression levels of hsa_circ_0091570 in HepG2 and SMMC-7721 cells were lower than that in LO2 cells (Fig. 2A). Next, the biological function of hsa_circ_0091570 was evaluated in human HCC cell lines. We constructed short interfering RNA (siRNA) and overexpressing plasmid targeting hsa_circ_0091570. After transfection, hsa_circ_0091570 expression was detected through qRT-PCR (Fig. 2B and C). It was indicated that down-regulated hsa_circ_0091570 significantly promoted the proliferation of HepG2 and SMMC-7721 cells through CCK-8 and EdU assays (Fig. 2D and E). In addition, cellular proliferation of stably transfected cells was assessed through colony formation assays, which supports the above results (Fig. 2F). Flow cytometry was used to evaluate the effect of hsa_circ_0091570 on apoptosis or cell cycle progression. The knockdown of hsa_circ_0091570 inhibited cell apoptosis in HepG2 and SMMC-7721 cells compared with the control group (Fig. 2G). In addition, hsa_circ_0091570 siRNA promoted cell cycle progression (Fig. 2H). Transwell and wound healing assay were performed to determine the promotion of cell migration by down-regulating hsa_circ_0091570 (Fig. 2I and J). The overexpression of hsa_circ_0091570 showed an opposite role in cell proliferation cell, apoptosis, and cell cycle (Fig. 2A–J).

3.3. hsa_circ_0091570 serves as a sponge for miR-1307

circRNAs can bind to miRNAs as a miRNA sponge and regulate gene expression [17]. The potential target miRNA of hsa_circ_0091570 was predicted through circinteractome. RNA in vivo precipitation was performed to determine the possible miRNAs that interact with hsa_circ_0091570 in HCC cells. Among these diverse miRNAs, we mainly

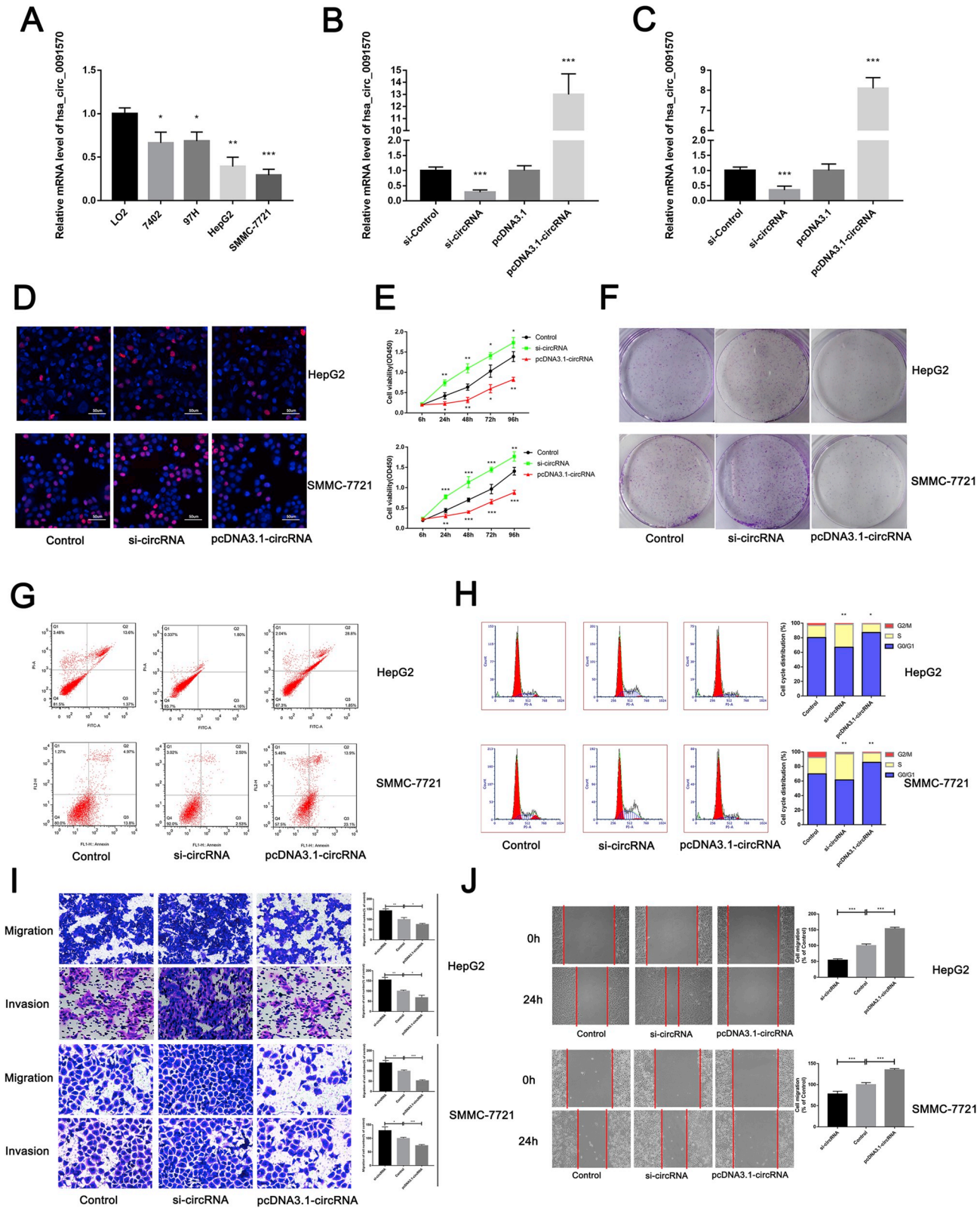

Fig. 2. Cytobiology change after treating cells with hsa_circ_0091570 siRNA. A: qRT-PCR is performed to verify the expression of hsa_circ_0091570 in HCC cell lines. B and C: HepG2(B) and SMMC-7721(C) cell lines are transfected with si-NC or si-hsa_circ_0091570 or overexpressing plasmid, and qRT-PCR analysis demonstrates that the transfection is successful. D: EDU assay is performed to evaluate cell proliferation. E: CCK8 assay is performed to assess cell growth. F: Colony formation assays are conducted in different treated cells. G and H: Flow cytometry is performed to indicate cell apoptosis (G) and cell cycle (H). I: Transwell assay is performed as described in the method. J: Migration of HepG2 and SMMC-7721 cells is detected by wound healing assay after transfection.

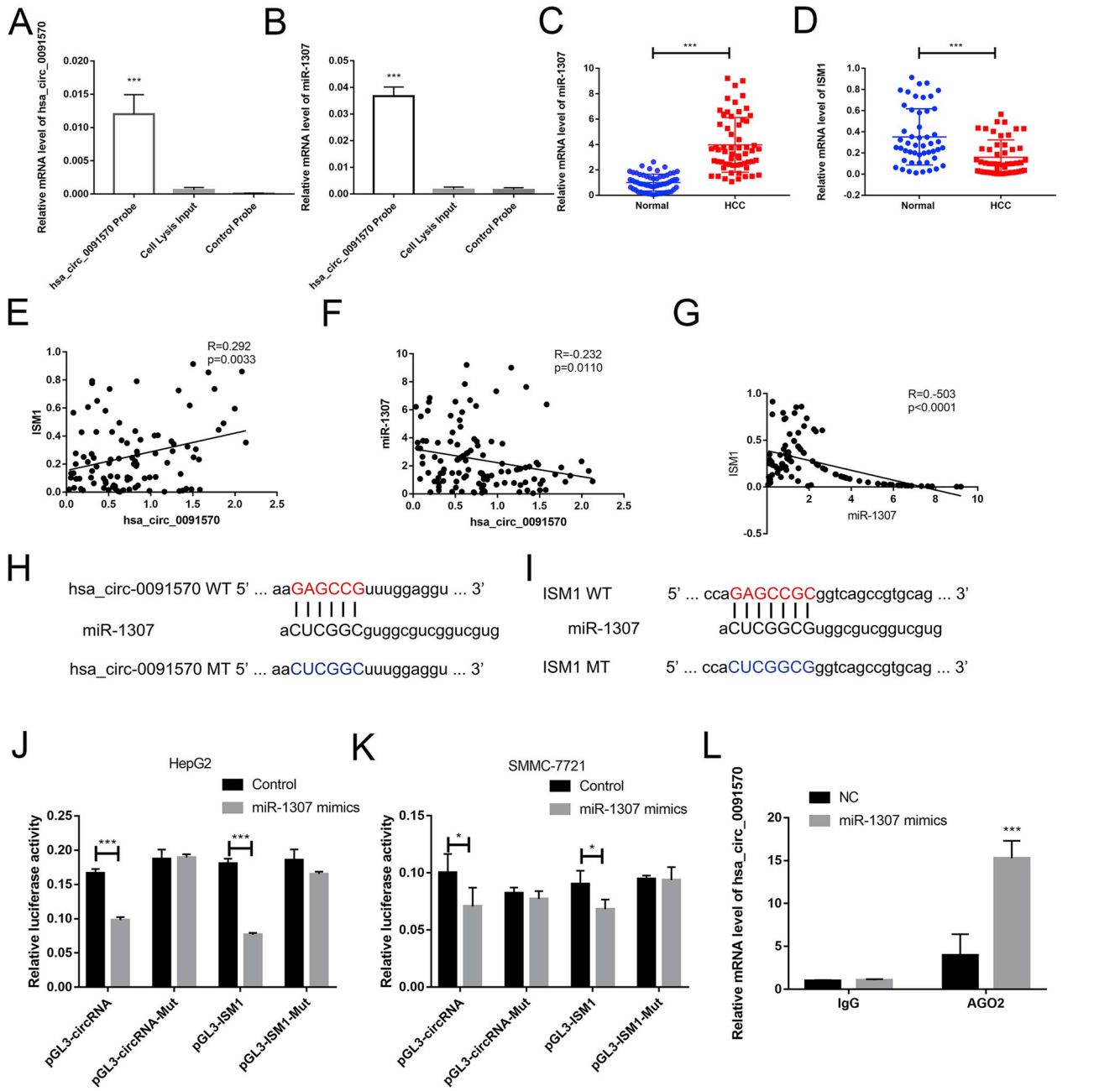

Fig. 3. hsa_circ_0091570 serves as a sponge for miR-1307. A: hsa_circ_0091570 in HCC cell lysis is pulled and enriched with hsa_circ_0091570 specific probe and detected through qPCR. B: miR-1307 is pulled and enriched with hsa_circ_0091570 specific probe and detected through qPCR. C: Relative expression of miR-1307 in HCC tissues compared with normal tissues. D: mRNA levels of ISM1 in HCC tissues and normal control samples are detected through qRT-PCR. E: Bivariate correlation analysis of the relationship between hsa_circ_0091570 and ISM1 expression level. F: Significant negative correlation is observed between the expression levels of hsa_circ_0091570 and miR-1307 in the same paired samples. G: Significant negative correlation is observed between the expression levels of ISM1 and miR-1307 in the same paired samples. H and I: Putative miRNA binding sites in the hsa_circ_0091570(H) and ISM1(I) sequence. Putative miRNA recognition sites are cloned downstream of the luciferase gene. Bottom: mutations in the hsa_circ_0091570(H) and ISM1(I) sequences to create the mutant luciferase reporter constructs. J and K: Luciferase reporter in HepG2(H) and SMMC-7721(I) cells. Luciferase activity is determined by using dual luciferase assay and is shown as the relative luciferase activity normalized to renilla activity. L: RIP experiments are performed using Ago2 and IgG antibodies to immunoprecipitate, and primers are used to detect hsa_circ_0091570.

examined 15 miRNAs that are closely related to cancer progression. The expression of hsa_circ_0091570 and its target miRNA, which were pulled from HCC cells, were analyzed through qRT-PCR. Specific enrichment of hsa_circ_0091570 in HCC cells was observed compared with input control. In addition, miR-1307 expression was significantly higher among these candidate miRNAs, which suggests that miR-1307 might be the potential target miRNA of hsa_circ_0091570 involved in HCC progression (Fig. 3A and B).

To investigate whether hsa_circ_0091570 could exert its role by binding to its target miRNA, the expression of miR-1307 in 60 pairs of HCC tissues and paired tissues was first detected through qRT-PCR. Thus, miR-1307 was up-regulated in HCC tissues (Fig. 3C). We used three algorithms (DIANA [23], miRanda [24], and PITA [25]) to determine the assumed target genes of miR-1307 in HCC and predicted ISM1. ISM1 was suggested to potently suppress xenograft tumor growth and angiogenesis in mice [26]. mRNA expression level of ISM1

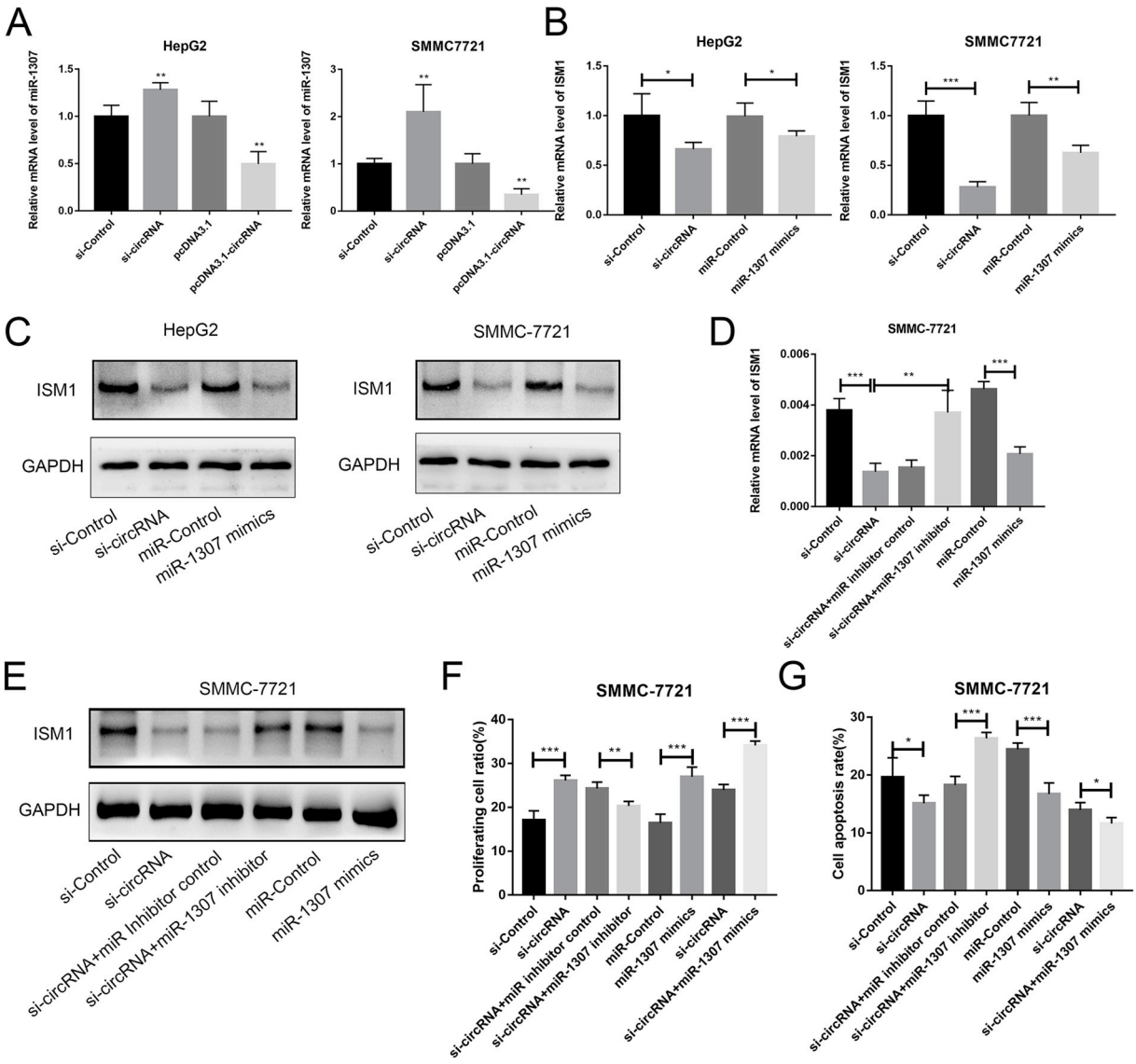

Fig. 4. hsa_circ_0091570 suppresses tumor progression by sponging miR-1307 and up-regulating ISM1 expression A: HepG2 and SMMC-7721 cell lines are transfected with si-NC or si-hsa_circ_0091570 or overexpressing plasmid, and qRT-PCR is used to detect the expression of miR-1307. B: HepG2 and SMMC-7721 cell lines are treated with si-NC or si-hsa_circ_0091570 or miR-1307 mimics, and qRT-PCR is used to detect the expression of ISM1. C: The protein level of ISM1 is detected through Western Blot after treatment. D–G: After silencing hsa_circ_0091570, miR-1307 inhibitor is added to SMMC-7721 cell culture. ISM1 expression in mRNA level is measured by qRT-PCR(D). E: ISM1 protein expression level is analyzed through Western blot. F: Proliferation ratio of HCC cells is measured by EdU incorporation. G: Apoptosis ratio of HCC cells is measured by FACS.

increased in HCC compared with the normal controls (Fig. 3D). In addition, significant correlation was observed on the expression levels of hsa_circ_0091570, miR-1307, and ISM1 (Fig. 3E–G). To ensure the interaction of hsa_circ_0091570 and miR-1307, miR-1307 and ISM1, luciferase reporter plasmids with mutant or wild type hsa_circ_0091570 or ISM1 sequence were co-transfected with miR-1307 mimics or negative control. The luciferase activity was significantly lower in miR-1307 mimic group (Fig. 3J and K). We used AGO2 RIP assay to ensure the sponge role of hsa_circ_0091570. It was shown that hsa_circ_0091570 was highly expressed in the AGO2 group than those in input control (Fig. 3L). These data confirmed that hsa_circ_0091570 could act as a sponge for miR-1307 and regulate ISM1 expression.

3.4. hsa_circ_0091570 suppresses tumor progression by sponging miR-1307 and up-regulating ISM1 expression

We detected the expression level of miR-1307 after silencing or overexpressing hsa_circ_0091570 to determine whether hsa_circ_0091570 could suppress HCC progression by sponging miR-1307. hsa_circ_0091570 knockdown could increase the expression of miR-1307, and hsa_circ_0091570 over-expression could decrease the expression of miR-1307 (Fig. 4A). After transfecting hsa_circ_0091570 siRNA or miR-1307 mimics, the expression of ISM1, the target gene of miR-1307, was significantly reduced in HCC cell lines (Fig. 4B and C). Furthermore, the down-regulating effect of ISM1 could be relieved by the miR-1307 inhibitor (Fig. 4D). The protein expression file confirmed these results (Fig. 4E). miR-1307 down-regulation could reverse the promotion of proliferation and inhibition of apoptosis of HCC cells induced by hsa_circ_0091570. By contrast, the effect of hsa_circ_0091570 on cell proliferation and apoptosis could be aggravated by miR-1307 over-expression (Fig. 4F and G). Thus, hsa_circ_0091570 exert its anti-tumor effect by protecting ISM1 from the down-regulation of miR-1307.

3.5. Knockdown of hsa_circ_0091570 in tumors accelerated HCC growth

SMMC-7721 cells transfected with scrambled or hsa_circ_0091570

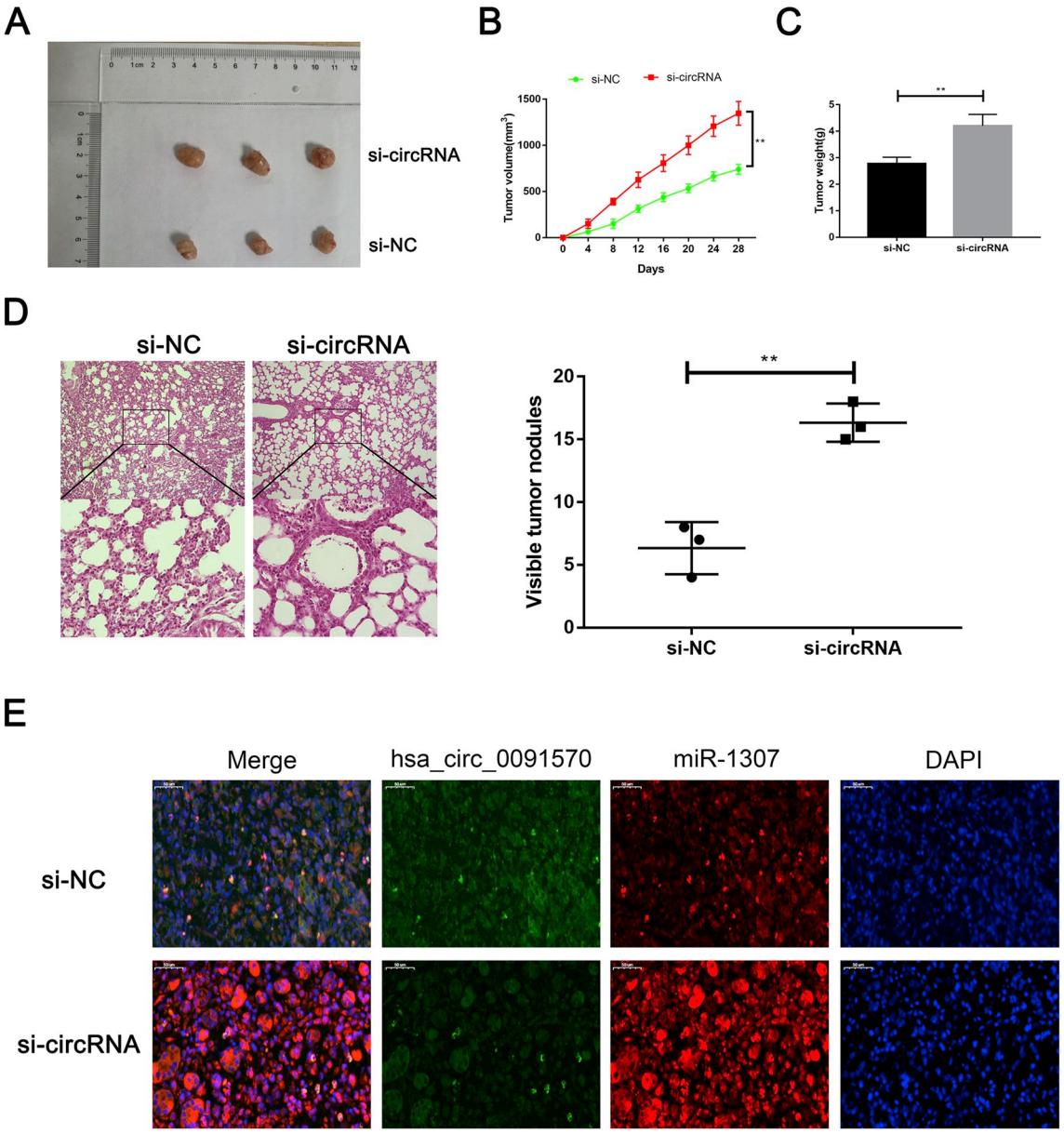

Fig. 5. Knockdown of hsa_circ_0091570 in tumors accelerated HCC growth. A: Representative images of xenografts tumor (three mice per group) in nude mice. B: Tumor volume is monitored every 4 days for 28 days. C: The weights of xenograft tumors are summarized. D: Representative images of HE stained lung metastatic nodules are shown. The number of metastatic nodules is quantified in the right panel. E: miR-1307 co-localized with hsa_circ_0091570 in xenografts tumor of si-NC or si-hsa_circ_0091570 group is detected by FISH.

siRNAs were subcutaneously injected into nude mice to investigate the role of hsa_circ_0091570 in HCC tumor growth in vivo. The knockdown of hsa_circ_0091570 increased the tumor volume and tumor weight (Fig. 5A–C) following the four-week intratumorally injections. Furthermore, immunohistochemistry ascertained that mice with hsa_circ_0091570 siRNAs had numerous visible metastatic nodules (Fig. 5D). These results were consistent with the in vitro results. These results above were consistent with those in vitro. Then we carried out FISH analysis and showed that hsa_circ_0091570 was decreased and miR-1307 was increased by siRNA, and they all expressed in cytoplasm (Fig. 5E).

3.6. Intratumoral knockdown of hsa_circ_0091570 enhances HCC growth in vivo

To elucidate the role of hsa_circ_0091570 in HCC growth in vivo, SMMC-LTNM mice, which showed similar manifestations to the clinical progression of HCC, were used in the experiment. After the two-week intratumorally injection of cholesterol-conjugated hsa_circ_0091570 siRNAs, the tumor volume, serum AFP, cell proliferation, and invasion marker were analyzed. The tumor volume of SMMC-LTNM mice with hsa_circ_0091570 siRNA injection was higher than those injected with negative control (Fig. 6A). Similarly, AFP was high in sera of hsa_circ_0091570 siRNA-injected mice (Fig. 6B). Based on the experimental results in vitro, hsa_circ_0091570 and ISM1 expression in tumor tissues were markedly decreased by the intratumorally injection of hsa_circ_0091570 siRNA (Fig. 6C). Immunohistochemistry was employed to detect the expression of ISM1 in the tumor tissues, and the expression accorded with mRNA expression. Further, MMP2 and PCNA, as the markers of cell proliferative and invasive capacity, were enhanced by silencing hsa_circ_0091570 (Fig. 6D). On this basis, we identify hsa_circ_0091570 as a suppressor of HCC progression in vivo (see Fig. 7).

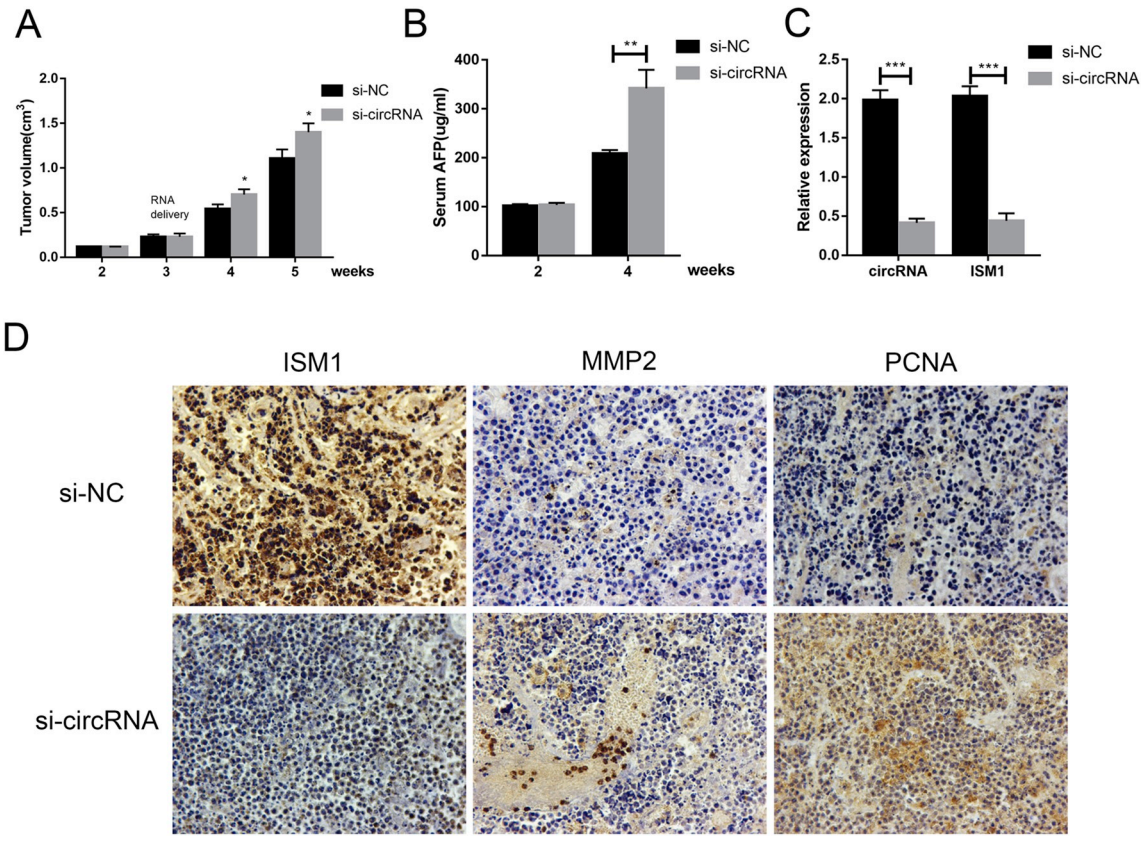

Fig. 6. Intratumoral knockdown of hsa_circ_0091570 enhances HCC growth in vivo. A: Effect of intratumorally hsa_circ_0091570 knockdown on tumor growth in SMMC-LTNM mice. B: Effects of intratumoral hsa_circ_0091570 knockdown on AFP level of SMMC-LTNM HCC-bearing nude mice. AFP is detected by ELISA after intratumoral injection of cholesterol-modified hsa_circ_0091570 siRNA, control siRNA. C: The expression of hsa_circ_0091570 and ISM1 in SMMC-LTNM tumor tissue 48 h after intratumoral injection of cholesterol-modified treatment. D: Immunostaining of ISM1, MMP2, and PCNA expression in SMMC-LTNM tumor tissues after intratumoral hsa_circ_0091570 knockdown at the fifth week.

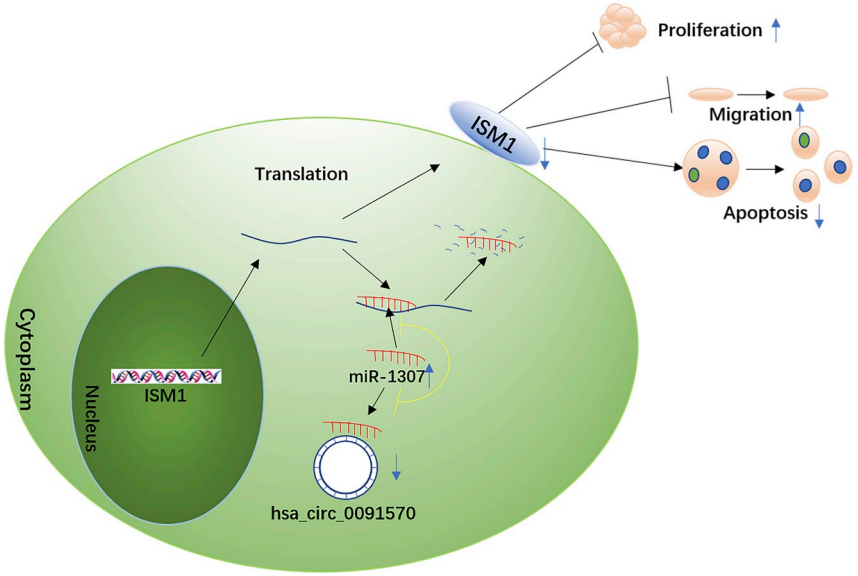

Fig. 7. Low expression of hsa_circ_0091570 increases the level of miR-1307, which decreases the expression level of ISM1, thus stimulates cell proliferation and migration and suppresses apoptosis in HCC.

4. Discussion

CircRNAs are a type of ncRNA that are newly discovered and commonly exist in various species [27]. Moreover, circRNAs are important in regulating gene transcription and expression, thus suggesting the vital functions of circRNAs in diverse biological and pathological processes [28]. Increasing studies have shown that circRNAs could be differently expressed and participate in tumor growth and progression of HCC [29]. The expression of circRNAs in HCC is significantly diverse. In our research, hsa_circ_0091570 was remarkably down-regulated by

microarrays and HCC tissues. Meanwhile, the expression level of this circRNA was considerably related to the tumor Edmondson Grade, metastasis, and prognosis of HCC patients, thus implying the potential role of hsa_circ_0091570 as a promising diagnostic marker for HCC. In addition, subsequent experiments in vitro showed that the down-regulation of hsa_circ_0091570 expression promotes cell proliferation and cell migration, and inhibits the apoptosis rate of HCC cell lines. Xenograft model results were consistent with those in vitro. All these findings implied that hsa_circ_0091570 might play a critical role in HCC progression.

miRNAs are a new class of short non-coding RNAs that can negatively regulate the expression of many target genes by interacting with the 3′-UTR in HCC [29]. miR-1307 is involved in the carcinogenesis of different cancers, such as colorectal cancer [30], breast cancer [31], and prostate cancer [32], and is related to the chemoresistance of cancer cells [33]. Furthermore, miR-1307 contributes to prostate cancer proliferation by targeting FOXO3A [32]. miR-1307 expression was regulated in HCC cells in our study. Furthermore, circRNAs are mainly considered a miRNA sponge and reverses the inhibitory effects of miRNA. In this study, miR-1307, as a target of hsa_circ_0091570, can serve as a ceRNA to regulate the downstream mRNA of miR-1307. RIP assay was employed to confirm the interaction of hsa_circ_0091570 and miR-1307.

ISM1 was initially identified as a gene that is closely related to embryonic development. Moreover, it was determined to have the capacity to block angiogenesis by VEGF, bFGF, serum-induced EC proliferation inhibition, and apoptosis promotion [26]. Mice injected with ISM1 proved the tumor-suppressing capacity of ISM1 [34]. The inhibition of hsa_circ_0091570 could down-regulate ISM1 expression in vitro and in mice that were intratumorally injected with hsa_circ_0091570 siRNA. The changed expression of ISM1 caused by hsa_circ_0091570 siRNA could be reversed by miR-1307 inhibitor, which accorded with the conversion of enhanced cell proliferation and low apoptosis rate in HCC cell lines. Similar results were obtained by intratumorally injection of cholesterol-conjugated hsa_circ_0091570 siRNA in SMMC-LTNM mice in terms of tumor volume, AFP, and proliferation and invasion-related gene expression.

In summary, hsa_circ_0091570 is down-regulated in HCC and could function as a ceRNA by sponging miR-1307 to regulate the expression of ISM1 and participate in HCC progression. These data suggest that hsa_circ_0091570 is a new potential target for prognosticating and effectively treating HCC.

Author contributions

Study design: BZ and MS; Perform the experiment: YW, TW, MD, SX and MS; Data collection and analysis: YW, TW, MD and SX; Drafting of the manuscript: YW, TW and MS; Manuscript revision: BZ; Final approval: all authors.

Conflicts of interest

All of the contributors in this study declared no conflict of interest.

Acknowledgement

None.

Appendix A. Supplementary data

Supplementary data to this article can be found online at https://doi.org/10.1016/j.canlet.2019.06.007.

References

[1] L.A. Torre, F. Bray, R.L. Siegel, J. Ferlay, J. Lortet-Tieulent, A. Jemal, Global cancer statistics, Ca - Cancer J. Clin. 65 (2012) 87–108 2015.
[2] J. Ferlay, I. Soerjomataram, R. Dikshit, S. Eser, C. Mathers, M. Rebelo, D.M. Parkin, D. Forman, F. Bray, Cancer incidence and mortality worldwide: sources, methods and major patterns in GLOBOCAN 2012, Int. J. Cancer 136 (2015) E359–E386.
[3] K.O. Nielsen, K.S. Jacobsen, A.H. Mirza, T.N. Winther, J. Storling, D. Glebe, F. Pociot, B. Hogh, Hepatitis B virus upregulates host microRNAs that target apoptosis-regulatory genes in an in vitro cell model, Exp. Cell Res. 371 (2018) 92–103.
[4] S.H. Lee, S.K. Hyun, H.B. Kim, C.D. Kang, S.H. Kim, Potential role of CD133 expression in the susceptibility of human liver cancer stem-like cells to TRAIL, Oncol. Res. 24 (2016) 495–509.
[5] F. Dionisi, E. Ben-Josef, The use of proton therapy in the treatment of gastrointestinal cancers: liver, Cancer J. 20 (2014) 371–377.
[6] R.A. Hlady, K.D. Robertson, A three-pronged epigenetic approach to the treatment of hepatocellular carcinoma, Hepatology 68 (4) (2018) 1226–1228, https://doi.org/10.1002/hep.30133.
[7] A. Villanueva, V. Hernandez-Gea, J.M. Llovet, Medical therapies for hepatocellular carcinoma: a critical view of the evidence, Nat. Rev. Gastroenterol. Hepatol. 10 (2013) 34–42.
[8] L.L. Chen, L. Yang, Regulation of circRNA biogenesis, RNA Biol. 12 (2015) 381–388.
[9] Y. Liu, Y. Dong, L. Zhao, L. Su, J. Luo, Circular RNAMTO1 suppresses breast cancer cell viability and reverses monastrol resistance through regulating the TRAF4/Eg5 axis, Int. J. Oncol. 53 (2018) 1752–1762.
[10] J. Liu, D. Wang, Z. Long, J. Liu, W. Li, CircRNA8924 promotes cervical cancer cell proliferation, migration and invasion by competitively binding to MiR-518d-5p/519-5p family and modulating the expression of CBX8, Cell. Physiol. Biochem. 48 (2018) 173–184.
[11] H. Cai, B. Hu, L. Ji, X. Ruan, Z. Zheng, Hsa_circ_0103809 promotes cell proliferation and inhibits apoptosis in hepatocellular carcinoma by targeting miR-490-5p/SOX2 signaling pathway, Am J Transl Res 10 (2018) 1690–1702.
[12] Z. Guan, J. Tan, W. Gao, X. Li, Y. Yang, X. Li, Y. Li, Q. Wang, Circular RNA hsa_circ_0016788 regulates hepatocellular carcinoma tumorigenesis through miR-486/CDK4 pathway, J. Cell. Physiol. 234 (1) (2018) 500–508, https://doi.org/10.1002/jcp.26612.
[13] L. Fu, Z. Jiang, T. Li, Y. Hu, J. Guo, Circular RNAs in hepatocellular carcinoma: functions and implications, Cancer Med (2018 Jun 1), https://doi.org/10.1002/cam4.1574.
[14] D. Chen, C. Zhang, J. Lin, X. Song, H. Wang, Screening differential circular RNA expression profiles reveal that hsa_circ_0128298 is a biomarker in the diagnosis and prognosis of hepatocellular carcinoma, Cancer Manag. Res. 10 (2018) 1275–1283.
[15] M.W. Lin, Y.W. Tseng, C.C. Shen, M.N. Hsu, J.R. Hwu, C.W. Chang, C.J. Yeh, M.Y. Chou, J.C. Wu, Y.C. Hu, Synthetic switch-based baculovirus for transgene expression control and selective killing of hepatocellular carcinoma cells, Nucleic Acids Res. 46 (2018) e93.
[16] S. Meng, H. Zhou, Z. Feng, Z. Xu, Y. Tang, P. Li, M. Wu, CircRNA: functions and properties of a novel potential biomarker for cancer, Mol. Cancer 16 (2017) 94.
[17] J. Hu, P. Li, Y. Song, Y.X. Ge, X.M. Meng, C. Huang, J. Li, T. Xu, Progress and prospects of circular RNAs in Hepatocellular carcinoma: novel insights into their function, J. Cell. Physiol. 233 (2018) 4408–4422.
[18] L. Salmena, L. Poliseno, Y. Tay, L. Kats, P.P. Pandolfi, A ceRNA hypothesis: the Rosetta Stone of a hidden RNA language? Cell 146 (2011) 353–358.
[19] Y. Liu, C. Lu, Y. Zhou, Z. Zhang, L. Sun, Circular RNA hsa_circ_0008039 promotes breast cancer cell proliferation and migration by regulating miR-432-5p/E2F3 axis, Biochem. Biophys. Res. Commun. 502 (2018) 358–363.
[20] X. Su, H. Wang, W. Ge, M. Yang, J. Hou, T. Chen, N. Li, X. Cao, An in vivo method to identify microRNA targets not predicted by computation algorithms: p21 targeting by miR-92a in cancer, Cancer Res. 75 (2015) 2875–2885.
[21] J. Hou, L. Lin, W. Zhou, Z. Wang, G. Ding, Q. Dong, L. Qin, X. Wu, Y. Zheng, Y. Yang, W. Tian, Q. Zhang, C. Wang, Q. Zhang, S.M. Zhuang, L. Zheng, A. Liang, W. Tao, X. Cao, Identification of miRNomes in human liver and hepatocellular carcinoma reveals miR-199a/b-3p as therapeutic target for hepatocellular carcinoma, Cancer Cell 19 (2011) 232–243.
[22] X.P. Zhang, Y.B. Jiang, C.Q. Zhong, N. Ma, E.B. Zhang, F. Zhang, J.J. Li, Y.Z. Deng, K. Wang, D. Xie, S.Q. Cheng, PRMT1 promoted HCC growth and metastasis in vitro and in vivo via activating the STAT3 signalling pathway, Cell. Physiol. Biochem. 47 (2018) 1643–1654.
[23] M.D. Paraskevopoulou, G. Georgakilas, N. Kostoulas, M. Reczko, M. Maragkakis, T.M. Dalamagas, A.G. Hatzigeorgiou, DIANA-LncBase: experimentally verified and computationally predicted microRNA targets on long non-coding RNAs, Nucleic Acids Res. 41 (2013) D239–D245.
[24] D. Betel, M. Wilson, A. Gabow, D.S. Marks, C. Sander, The microRNA.org resource: targets and expression, Nucleic Acids Res. 36 (2008) D149–D153.
[25] K. Qu, S. Garamszegi, F. Wu, H. Thorvaldsdottir, T. Liefeld, M. Ocana, D. Borges-Rivera, N. Pochet, J.T. Robinson, B. Demchak, T. Hull, G. Ben-Artzi, D. Blankenberg, G.P. Barber, B.T. Lee, R.M. Kuhn, A. Nekrutenko, E. Segal, T. Ideker, M. Reich, A. Regev, H.Y. Chang, J.P. Mesirov, Integrative genomic analysis by interoperation of bioinformatics tools in GenomeSpace, Nat. Methods 13 (2016) 245–247.
[26] W. Xiang, Z. Ke, Y. Zhang, G.H. Cheng, I.D. Irwan, K.N. Sulochana, P. Potturi, Z. Wang, H. Yang, J. Wang, L. Zhuo, R.M. Kini, R. Ge, Isthmin is a novel secreted angiogenesis inhibitor that inhibits tumour growth in mice, J. Cell Mol. Med. 15 (2011) 359–374.
[27] S.J. Conn, K.A. Pillman, J. Toubia, V.M. Conn, M. Salmanidis, C.A. Phillips, S. Roslan, A.W. Schreiber, P.A. Gregory, G.J. Goodall, The RNA binding protein quaking regulates formation of circRNAs, Cell 160 (2015) 1125–1134.

[28] D.B. Dudekula, A.C. Panda, I. Grammatikakis, S. De, K. Abdelmohsen, M. Gorospe, CircInteractome: a web tool for exploring circular RNAs and their interacting proteins and microRNAs, RNA Biol. 13 (2016) 34–42.
[29] M. Wang, F. Yu, P. Li, Circular RNAs: characteristics, function and clinical significance in hepatocellular carcinoma, Cancers 10 (2018).
[30] R. Tang, Q. Qi, R. Wu, X. Zhou, D. Wu, H. Zhou, Y. Mao, R. Li, C. Liu, L. Wang, W. Chen, D. Hua, H. Zhang, W. Wang, The polymorphic terminal-loop of pre-miR-1307 binding with MBNL1 contributes to colorectal carcinogenesis via interference with Dicer1 recruitment, Carcinogenesis 36 (2015) 867–875.
[31] F. Cordero, G. Ferrero, S. Polidoro, G. Fiorito, G. Campanella, C. Sacerdote, A. Mattiello, G. Masala, C. Agnoli, G. Frasca, S. Panico, D. Palli, V. Krogh, R. Tumino, P. Vineis, A. Naccarati, Differentially methylated microRNAs in prediagnostic samples of subjects who developed breast cancer in the European Prospective Investigation into Nutrition and Cancer (EPIC-Italy) cohort, Carcinogenesis 36 (2015) 1144–1153.
[32] X. Qiu, Y. Dou, miR-1307 promotes the proliferation of prostate cancer by targeting FOXO3A, Biomed. Pharmacother. 88 (2017) 430–435.
[33] W.T. Chen, Y.J. Yang, Z.D. Zhang, Q. An, N. Li, W. Liu, B. Yang, MiR-1307 promotes ovarian cancer cell chemoresistance by targeting the ING5 expression, J. Ovarian Res. 10 (2017) 1.
[34] M. Chen, Y. Zhang, V.C. Yu, Y.S. Chong, T. Yoshioka, R. Ge, Isthmin targets cell-surface GRP78 and triggers apoptosis via induction of mitochondrial dysfunction, Cell Death Differ. 21 (2014) 797–810.